https://doi.org/10.3311/PPch.18953

Periodica Polytechnica Chemical Engineering

Effect of Mixed Oxide-Based TiO_2 on the Physicochemical Properties of Chitosan Films

Luis Miguel Anaya-Esparza[1,2], Apolonio Vargas-Torres[3], Heidi María Palma-Rodríguez[3], Marisol Patricia Castro-Mendoza[3], Elhadi M. Yahia[4], Alejandro Pérez-Larios[2*], Efigenia Montalvo-González[1*]

[1] Integral Food Research Laboratory, Technological Institute of Tepic, Avenida Tecnologico 2595, 63175 Tepic, Mexico
[2] Department of Livestock and Agricultural Sciences, University Center of Los Altos of the University of Guadalajara, Av. Rafael Casillas Aceves 1200, 47600 Tepatitlán de Morelos, Mexico
[3] Food Science and Technology Research Center, Institute of Agricultural Sciences, Autonomous University of the State of Hidalgo, Abasolo 600, 42039 Pachuca, Mexico
[4] Faculty of Natural Sciences, Autonomous University of Queretaro, Avenida de las Ciencias S/N, 76230 Juriquilla, Mexico
[*] Corresponding authors, e-mails: emontalvo@ittepic.edu.mx; alarios@cualtos.udg.mx

Received: 17 July 2021, Accepted: 26 November 2021, Published online: 27 January 2022

Abstract

The physicochemical, mechanical, and structural properties of chitosan-based films (CS) alone or CS-films with mixed oxide nanoparticles (TiO_2-ZnO-MgO, TZM; CSTZM) at different concentrations (125, 250, and 500 μg mL^{-1}) were investigated. The addition of nano-TZM promoted a color change (from colorless to white) in the film-forming solution, which increased its turbidity and it decreased viscosity. CSTZM were semitransparent (transmittance, *T*% decreased up to 49%) compared to CS-based films (*T*% = 95.5). CSTZM (particularly at a concentration of 500 μg mL^{-1}) exhibited an improvement in the moisture content (decreased from 12.6 to 9.67%), water solubility (decreased from 14.94 to 10.22%), degree of swelling (increased from 19.79 to 36.28%), water vapor barrier (decreased from 6.62 x 10^{-16} to 4.33 x 10^{-16} g m^{-1} h^{-1} Pa^{-1}), thermal stability (the endotherm peak increased from 99.5 to 157.7 °C), and mechanical properties (tensile strength and elongation at break increased from 4.15 to 4.98 kPa and 6.96 to 56.18%, respectively, while the modulus of elasticity decreased from 144 kPa to 4.11 kPa), without toxicity effects on Artemia salina (93.33% survival). X-ray diffraction and Fourier transform infrared studies demonstrated an interaction between CS-based films and nano-TZM. Overall, this film exhibited great potential for diverse industrial applications.

Keywords

chitosan, titanium dioxide, mixed-oxide systems, nanoparticles, hybrid composites

1 Introduction

Developing hybrid materials has gained considerable attention in the last years, mainly due to their interesting properties for several industrial and biomedical applications [1, 2]. Hybrid composites comprise a combination of organic-organic, inorganic-inorganic, and organic-inorganic compounds [1, 2]. Recently, a particular interest has emerged in the use of natural polymers (gums, starch, and chitosan) with added inorganic (metallic or transition metal compounds) nanoparticles to obtain hybrid composites [3, 4], particularly for the chitosan-titanium dioxide-based hybrid composites [5].

Chitosan (CS) is a linear polysaccharide consisting of β-(1-4)-linked D-glucosamine and N-acetyl-D-glucosamine. It is obtained from chitin deacetylation (synthesized by chemical or enzymatic pathways), and it has been recognized as a biologically functional compound [6]. It is non-toxic and biodegradable with excellent antimicrobial and film-forming properties for many relevant applications (food preservation, biomedical and environmental applications) [7]. Furthermore, its poly-cationic character enhances its biocompatibility with other organic or inorganic compounds, mainly associated with the presence of functional groups ($-NH_2$ and $-OH$) in its structure [7]. Furthermore, the addition of TiO_2 nanoparticles to CS-based films improves their mechanical, physical, and biological properties [3, 5].

Cite this article as: Anaya-Esparza, L. M., Vargas-Torres, A., Palma-Rodríguez, H. M., Castro-Mendoza, M. P., Yahia, E. M., Pérez-Larios, A., Montalvo-González, E. "Effect of Mixed Oxide-Based TiO_2 on the Physicochemical Properties of Chitosan Films", Periodica Polytechnica Chemical Engineering, 2022. https://doi.org/10.3311/PPch.18953

Titanium dioxide (TiO_2) is a multipurpose material with interesting physicochemical and technological properties (amphoteric, inert, non-toxic, chemical and thermal stability, compatible with organic and inorganic compounds). It exhibits antimicrobial, adsorptive, and photocatalytic properties, and it is used in wastewater treatment, biomedical, pharmaceutical, and food applications, in compliance with the recommended safe dosage [8]. TiO_2 is widely used as a pharmaceutical or food additive, for example, as a white colorant (Code of Federal Regulations 21CFR73.575 of U.S. Food and Drug Administration), where its concentration must not exceed 1% by weight of pharmaceutical or food product [9]. However, at high doses (1000 mg kg^{-1} body weight per day), TiO_2 may exert toxic effects, mainly by its accumulation in the body due to a long half-life [10]. On the other hand, the use of TiO_2 is acceptable (without limitations) for the development of polymeric coatings for pharmaceutical or food packaging applications (Code of Federal Regulations 21CFR175.300 of U.S. FDA) [11]. Recently, TiO_2 has been used as a reinforcement agent of biopolymer-based materials, enhancing their functional and technological properties [3, 5].

Chitosan-TiO_2 (CST) composites and their potential applications have been explored in the last decade [5, 12]. The most studied applications are antibacterial activity [13] and water pollutant degradation [14]. Biomedical applications of CST have also been widely investigated [15]. Furthermore, CST films have been applied for fruit preservation [16]. The addition of TiO_2 improves the technological and biological characteristics of CS-based films, with a better performance of CS-based films properties observed when TiO_2 nanoparticles were previously doped with other compounds (i.e., CS-TiO_2: Cu, CS-TiO_2: Ag, TiO_2: Au, TiO_2: Fe) [17–20]. Recently, we have reported that the TiO_2-based ternary mixed oxide system (TiO_2–ZnO–MgO) containing Zn (5%) and Mg (5%) exhibited improved structural and textural properties [21]. We have also observed significant antibacterial activity against pathogenic bacteria (*Staphylococcus aureus*, *Salmonella paratyphi*, *Listeria monocytogenes*, and *Escherichia coli*) without toxic effects on *Artemia salina* compared to undoped-TiO_2 nanoparticles [22]. There are no reports on the technological properties of CS-based films with the addition of a ternary mixed oxide-based TiO_2. Therefore, the main objective of this study was to investigate the efficiency of TiO_2–ZnO–MgO mixed oxide as reinforcement agent on CS-based films and their effects on the structural (Fourier transform infrared and X-ray diffraction studies), optical (color, opacity, and light transmittance), mechanical (elastic modulus, elongation at break, and tensile strength), thermal (differential scanning calorimetry studies), and water resistance (water vapor permeability, water solubility, and swelling index) properties, and their toxicity on *Artemia salina*.

2 Experimental details

Preparation of chitosan–TiO_2–ZnO–MgO hybrid films: The hybrid films were developed by the evaporative casting method according to the methodology described by Yong et al. [23] with some modifications. The chitosan (CS, medium molecular weight, Sigma Aldrich Chemical Company, St. Louis, MO, USA) film-forming solution was prepared (1 g CS dissolved in 95 mL of 1% acetic acid solution) under continuous magnetic stirring at 25 °C until the chitosan dissolved completely. Then, the pH of the solution was adjusted to 4.8 using NaOH (1 M) [24]. Subsequently, TiO_2–ZnO–MgO (TZM, containing 5% of Zn and 5% of Mg) mixed oxide (at 500, 250, and 125 μg mL^{-1}, respectively) nanoparticles (23 nm) were added to the chitosan solution to elaborate hybrid films (CSTZM). The mixed oxide was previously dissolved in 5 mL of 1% acetic acid solution and sonicated (FisherbrandTM, CPX1800 Ultrasonic bath, Branson Korea Co., Ltd. South Korea) for 5 min to avoid aggregations. Afterward, 15% (by weight of total solids) of glycerol (as plasticizer agent) on the film-forming solution was added with continuous magnetic stirring for 20 min [24]. The resultant solution was then deposited onto a Petri dish (90 × 15 mm) and allowed to dry at 37 °C for 24 h [23]. Pure CS and CS-titanium dioxide nanoparticles (CST) films were used as controls and prepared with the same procedure as described previously. The films were stored for later tests. TZM and TiO_2 nanoparticles were synthesized by the Sol-gel method (using titanium-(IV) butoxide, magnesium di-ter-butoxide, and zinc nitrate as precursors) and exhibited near-spherical shapes with mean sizes of 17 to 23 nm [21, 22]. For identification, the films were labeled as CSTZM-X or CST-X, where X is the TZM or TiO_2 wt. content (i.e., CSTZM-125 contain 125 μg mL^{-1} of CS solution).

2.1 Film-forming solution and hybrid film characterization

The viscosity of film-forming solution: The viscosity of CSTZM film-forming solution was measured with a Rapid-Visco Analyzer (RVA-4, Newport Scientific, Sydney, Australia) according to Chen et al. [25] with

some modifications. The film-forming solution (30 mL) was stirred at 960 rpm and 30 °C for 10 s, then decreased to 160 rpm, and the solution heated to 80 °C for 5 min. After equilibrium was maintained for 5 min, the temperature was reduced to 30 °C in 5 min. The viscosity was expressed as Pa × second.

Turbidity of film-forming solution: The turbidity of film-forming solution from CSTZM was measured with a HACH 2100N Turbidimeter (Loveland, Colorado, USA) using a sample cell (95 mm high × 25 mm diameter) at room temperature according to the manufacturer instructions, and results were expressed as nephelometric turbidity units (NTU).

Film thickness: The thickness of CSTZM films was determined using a manual digital micrometer (Digimatic micrometer, 0.001 mm, Mitutoyo Co., Kobe, Japan). The thickness values were the average of ten measurements from 5 random locations on each film sample [26].

The moisture content of chitosan-based films: For the measurement of moisture content (*MC*), the CSTZM film sample (3 × 3 cm) was first equilibrated in a desiccator at room temperature for 48 h, and then dried in an oven at 105 °C to a constant weight [26]. The *MC* was calculated using the Eq. (1):

$$MC(\%) = \left[(Mi - Mf)/(Mi) \right] \times 100, \quad (1)$$

where *Mi* and *Mf* are the initial and final weights of the sample, respectively.

Water solubility (*WS*) of chitosan-based films: the *WS* of the CSTZM film was measured according to the methodology described by Zhang et al. [26]. For this, the equilibrated sample (3 × 3 cm) was immersed in a phosphate buffer solution (0.1 M, pH 7) for 24 h at 25 °C. The film was then dried at 105 °C until it reached a constant weight. Water solubility was calculated according to Eq. (2):

$$WS(\%) = \left[\left(Mi \times (1 - MC) - Mf \right) / \left(Mi \times (1 - MC) \right) \right], \quad (2)$$

where *Mi* and *Mf* are the initial and final weights of the film sample at 25 °C, respectively, and *MC* is the film moisture content obtained from Eq. (1).

Swelling of chitosan-based films: the swelling studies were performed according to Kavitha et al. [27] with some modifications. An equilibrated CSTZM film sample (3 × 3 cm) was immersed in a phosphate buffer solution (PBS, 0.1 M, pH 7.4) at 25 °C, and films were placed in PBS for 7 days (the dry weight of the film, *Wo*, was recorded). Then, the films were removed at 1, 4, and 7 days intervals, and the adsorbed water was removed with filter paper, and wet weight (*Ww*) was recorded. The swelling degree (*SD*) of the chitosan-based films were calculated in terms of the amounts of absorbed water relative to the initial mass and expressed as a percentage using Eq. (3):

$$SD(\%) = \left[(Ww - W0)/(Ww) \right] \times 100, \quad (3)$$

where *Ww* is the wet weight and *W*0 is the initial weight.

Water vapor permeability (WVP) of chitosan-based films: The *WVP* test was carried out according to the standard ASTM E96–95 method [28]. The water vapor transmission rate of the CSTZM film sample (average transfer area 0.00282744 m^2) was measured using a cup method (cups of 6 cm in diameter provided with anhydrous silica gel) at 25 °C and 75% of relative humidity (using NaCl solution). The permeation cells were weighed every hour for 8 h, and the water vapor transport was determined by the weight increase of the permeation cell. The water vapor transmission rate (*WVTR*, g s^{-1} m^{2-1}) was calculated from the slope of weight versus time (g s^{-1}) curve by linear regression, divided by the transfer area (m^2), and the *WVP* (g m^{-1} s^{-1} Pa^{-1}) was calculated using Eq. (4):

$$WVP = WVTR \times \left[(\text{film thickness}) / (\Delta \text{pressure}) \right], \quad (4)$$

where the thickness of the film is m and the Δpressure in Pa.

Color of chitosan-based films: Color studies, including light transmittance and opacity of the CSTZM films, were performed according to Oleyaei et al. [29] and Nouri and Mohammadi Nafchi [30] methods with some modifications. The color attributes (Chrome, hue, luminosity, as well as *a** and *b** coordinates values) were performed using a portable colorimeter (Konica Minolta CR-400, Konica Minolta Inc., Osaka, Japan).

The UV-Visible (UV-Vis) absorption spectra of CSTZM films were recorded from 200 to 800 nm with a UV-Vis spectrophotometer (Shimadzu UV-2600, Tokyo, Japan). The optical properties (opacity values) of the films were calculated using Eq. (5), as suggested by Oleyaei et al. [29]:

$$\text{Opacity} = \text{film absorbance at 600 nm/thickness film.} \quad (5)$$

Differential scanning calorimetry studies: The thermal properties of the CSTZM films were examined by TA Instruments equipment (Q2000, Newcastle, DE, USA) at a temperature range of 30 to 200 °C, at a heating rate of 10 °C min^{-1}, under nitrogen purge gas. A 10±1 mg film sample was put into a sample dish, and the reference was an empty dish [29].

Mechanical properties: The mechanical properties (elongation at break, tensile strength, and elastic modulus) of the CSTZM films were determined by using a Brookfield texture analyzer (Brookfield CT3, Brookfield Engineering Labs, Inc., USA) equipped with a 25 kg load cell following the ASTM standard method D882-95a [31]. Rectangular specimens (8 cm in length and 1 cm in width) were cut and conditioned at 57±2% of relative humidity (using NaBr solution) at 25±1 °C for at least 72 h. The ends of the film were fixed in each of the subjection gauges, and the initial grip separation among the gauges was 6 cm with a speed of deformation of 1 mm s^{-1}. The tensile strength (Eq. (6)), elongation at break (Eq. (7)), and elastic modulus (Eq. (8)) were calculated from the slope of the linear portion of the force-deformation curve.

$$\text{Tensile strength}(\text{Pa}) = (F)/(A) \quad (6)$$

Where F is the maximum load (N), and A is the cross-sectional film area (m^2).

$$\text{Elongation at break}(\%) = (Lb/Lo)\times 100 \quad (7)$$

Where Lb is the length of the film after testing (mm) and Lo is the initial film length (mm).

$$\text{Elastic modulus}(\text{Pa}) = (\Delta F/A)\times(\Delta L/Lo) \quad (8)$$

Where: ΔF and ΔL are the change in force and length in the film during initial linear deformation.

Structural studies: X-ray diffraction spectra of the hybrid films were obtained using an X-ray diffractometer (Empyrean, Malvern, Panalytical, Almelo, The Netherland) utilizing CuKα radiation (λ = 0.154 nm) from 10 to 90° (2θ degree). The Fourier transform infrared (FTIR) spectrum for the films was examined with an attenuated total reflectance FTIR spectrometer (Nicolet iS5, ThermoFisher Scientific, Tokyo, Japan). The spectrum was recorded at 25 °C in the range 4000 to 500 cm^{-1}.

Toxicity assay: The acute toxicity of CSTZM films was carried out using Artemia salina with three weeks of growth in artificial seawater (25 g L^{-1}) under recommended conditions [22, 32]. Ten specimens were placed in contact (test tubes containing 10 mL of saline water at 25 g L^{-1}) with the CSTZM film at different concentrations (0.5, 1.0, 2.0, and 4.0 mg mL^{-1}) at 28 °C in darkness [33]. After 24 h of exposition, the number of dead individuals (organisms that did not present any movements during one min of observation) were counted in each tube [34]. Test tubes with saline solution and tubes with the corresponding concentration of CS and CST films were used as negative controls, while tubes with dimethyl sulfoxide (DMSO, 0.5 mL mL^{-1}) were used as a positive control [35]. Results were expressed as the percentage of mortality [36], calculated using the Eq. (9):

$$\text{Mortality}(\%) = \left[\left(\sum CLL - \sum TLL\right)/\left(\sum CLL\right)\right]\times 100, \quad (9)$$

where CLL is control living larvae, and TLL is treated living larvae.

2.2 Statistical analysis

Results were expressed as mean ± standard deviation obtained from three independent experiments, and each sample was performed in triplicate, except for thickness, tensile strength, elongation at break, and elastic modulus, where at least ten measurements were made on each film sample. The data of all variables were subjected to a one-way ANOVA/Tukey test. Additionally, multivariate statistical tools like principal component analysis and hierarchical cluster analysis were performed to describe the correlations among variables and to estimate the relationship between CS and hybrid (CST and CSTZM) films. All analyses were done with Statistic software (v. 10 Statsoft®, Tulsa, OK, USA), using a significance level of α = 0.05.

3 Results and discussions

Fig. 1 illustrates the visual appearance of the CSTZM, CST, and CS film-forming solutions and their respective films [37]. The CS film-forming solution (Fig. 1) had a transparent and colorless form, indicating good solubility of chitosan in the acetic acid solution [8]. On the other hand, the film-forming solution of the CSTZM and CST showed color differences in a dose-dependent response (125 to 500 μg mL^{-1}) compared to the CS solution. The film-forming solution exhibited a color change from colorless to white, reducing the transparency of the solutions, which

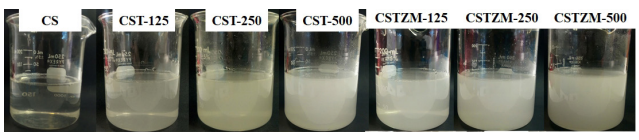

(a)

(b)

Fig. 1 Appearance of chitosan (CS), chitosan-TiO_2 ($CSTiO_2$), and chitosan-TZM (CSTZM) film-forming solutions (a) and films (b)

influenced the coloration and transparency of the film (Fig. 1 (b)). These findings are in agreement with those reported by Díaz-Visurraga et al. [12], who demonstrated that chitosan solutions became whiter after the nano-TiO_2 powder addition, and the transparency of the films was decreased [38]. These visual changes (color and transparency) of the CSTZM film-forming solution and films may be related to the intrinsic properties of TiO_2 (mainly a component of TZM mixed oxide) [14], which is widely used in diverse industrial applications as a white pigment and/or for its excellent ultraviolet-light -barrier properties [37].

3.1 Viscosity and turbidity of the film-forming solution

Table 1 shows the effect of incorporating TZM (CSTZM-125, CSTZM-250, and CSTZM-500) on the viscosity of the CS-film-forming solution. The viscosity profile of CS-film-forming solution (0.147 Pa s) is consistent with previous reports for chitosan solutions at 1% w/v [25]. Nonetheless, the concentration-dependent decrease of CS-film-forming solution viscosity ($p < 0.05$) is clearly shown by the presence of TZM (0.107–0.083 Pa s) and TiO_2 (0.118–0.102 Pa s) nanoparticles, where the lowest viscosity (0.083 Pa s) values were due to the addition of nano-TZM at 500 μg mL^{-1} (CSTZM-500). The viscosity of film-forming solution is an important quality indicator during polysaccharide-based film production. A high viscosity solution is difficult to pour, thus forming non-uniform films with the presence of air bubbles, therefore affecting the film quality [39]. Tang et al. [24] reported a decrease in the CS-film-forming solution viscosity (from 7 to < 1 Pa s) by adding TiO_2 (from 5 to 20% in weight) nanoparticles, where lower viscosity values were obtained at higher TiO_2 concentrations. The decrease of the viscosity in the chitosan solution may be related to the pH of the solution, promoting protonation of the amine group (NH_2), which results in the relaxation and subsequent reorganization of the chitosan chain facilitated by the interaction between the mixed oxide-based TiO_2 (TZM) and NH_2 groups [40, 41]. On the other hand, the decrease in the viscosity as a function of the increased nano-TZM loading (125 to 500 μg mL^{-1}) could be attributed to a physical entanglement with the chitosan chains, leading to a reduction of the interaction between macromolecules in the film-forming solution system [23]. According to Li et al. [42], the optimal CS:TiO_2 concentration rate during film production is necessary to avoid higher viscosity solutions. Therefore, CSTZM film-forming solution could be a suitable alternative for the development of CS-based hybrid films.

CS-film-forming solution had a turbidity of 18.99 NTU (Table 1), which is consistent with previous reports [42]. A significant ($p < 0.05$) increase in the turbidity of the CS-film-forming solution was observed when TZM (192–968 NTU) and TiO_2 (142–643 NTU) nanoparticles were added to the chitosan solutions. Turbidity is an optical property that indicates the loss of transparency of any liquid due to suspended particles [43]. The differences in turbidity values between CSTZM and CST film-forming solutions can be attributed to increased charge densities, mainly due to the presence of Mg^{2+} ions in the ternary mixed oxide structure, which can contribute to increased turbidity in the solutions [15].

Table 1 Effect of adding TiO_2-ZnO-MgO nanoparticles on the viscosity and turbidity of film-forming solutions and film thickness

Treatments	Viscosity (Pa s)	Turbidity (NTU)	Film thickness (mm)
CS	0.147±0.001^{a}	18.99±0.23^{g}	81.91±0.99^{c}
CST-125	0.118±0.001^{b}	142.33±1.37^{f}	81.75±1.14^{c}
CST-250	0.110±0.001^{e}	299.08±2.40^{d}	91.58±1.37^{b}
CST-500	0.102±0.001^{c}	643.25±2.60^{b}	99.50±0.75^{a}
CSTZM-125	0.107±0.001^{d}	192.96±1.66^{e}	82.91±0.80^{c}
CSTZM-250	0.098±0.001^{e}	389.08±2.21^{c}	93.17±1.37^{b}
CSTZM-500	0.083±0.001^{f}	968.41±2.57^{a}	99.16±0.87^{a}

Values are the average ± standard deviation. Different letters (a-f) in each column indicate significant differences between treatments (ANOVA, Tuckey's post hoc test, $\alpha = 0.05$). With the letter "a" are denoted the highest determined value, and with the letter "f" the lowest value.
The values denoted with different letters are different with level of significance $p < 0.05$, meaning that 95% of the determined results differ.

3.2 Film thickness

The chitosan-based films with added TZM nanoparticles were successfully prepared using the evaporative casting technique. They were semitransparent with opaque nature and flexible [44], as shown in Fig. 1 (b). Table 1 lists the thickness of CS-based films with or without inorganic nanoparticles added. A significant ($p < 0.05$) increase in the film thickness (CS: 81.91 μm) was observed due to the incorporation of nano-TZM (from 82.91 to 99.16 μm) in a dose-dependent manner. Where the major thickness of the film was observed at higher TZM nanoparticle loading, but it was similar to the obtained by the addition of nano-TiO_2 (81.75 to 99.5 μm). These findings are in agreement with previous reports for the thickness (from 70 to ≤ 100 μm) of CS-based films with TiO_2 addition [44–46]. According to Lian et al. [47], the interaction between the chitosan matrix and nano-TZM can reduce the interspaces in the film network, influencing the film thickness [29], which is usually dependent on the solids content of the film [12].

3.3 Moisture content, water solubility, and swelling properties of hybrid chitosan films

A significant decrease ($p < 0.05$) of up to 23% in the moisture content of CS-based film (12.66%) was observed due to the addition of nano-TZM (from 11.91 to 9.67%) in a dose-dependent response (from 125 to 500 μg mL^{-1}), which was similar to those obtained by the addition of nano-TiO_2 (from 11.12 to 9.06%) (Fig. 2). A similar tendency in moisture content (15.2 to 11.4%) in a film composed of a mixture of polysaccharides (*k*-Carrageenan, xanthan gum, and gellan gum) by the addition of nano-TiO_2 (1–7% w/w) were previously reported [48]. Likewise, Li et al. [37] reported that the presence of TiO_2 might reduce the tendency of hydroxyl groups present in the chitosan structure to interact with water molecules, promoting the formation of a more compact structure. However, Zhang et al. [26] reported an increase in the moisture content (from 31.49 to 35%) in the CS-based film with the presence of TiO_2 (800 mg 100 mL^{-1}), which was attributed to the mesoporous character and absorptive properties of TiO_2 that allows water molecules to be absorbed and retained by the film.

Additionally, the presence of nano-TZM reduced the water solubility from 14.05 to 10.22% of CS-based films (14.94%) in a TZM dose-dependent response (Fig. 3). This parameter reflects the water-resistance of any biopolymer-based film because films with high water solubility are not suitable for applications in high humidity environments [26]. A similar tendency was reported for chitosan [26], starch [29], and starch-chitosan [49] based films when TiO_2 was added. Furthermore, it has been reported that the compatibility among chitosan matrix and nano-TiO_2 can promote the formation of Ti–O hydrogen bonds with

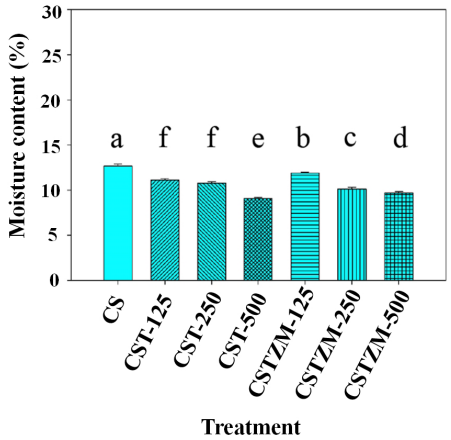

Fig. 2 Moisture content of chitosan-based films. Different letters in each column indicate significant statistical differences between treatments ($\alpha = 0.05$). See also the footnote of Table 1.

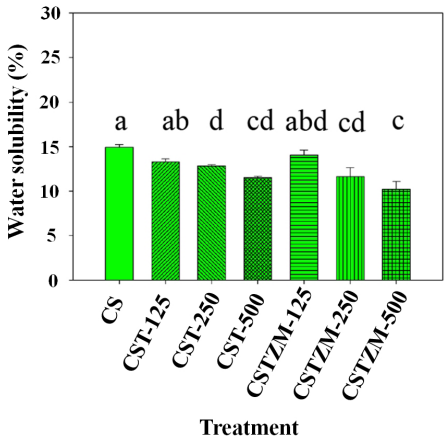

Fig. 3 Water solubility of chitosan-based films. Different letters in each column indicate significant statistical differences between treatments ($\alpha = 0.05$). See also the footnote of Table 1.

–OH and $–NH_2$ functional groups, reinforcing the composite structure that restricts the movement of the polymer and inorganic particles, promoting an increase in water tolerance [50]. The moisture content and water solubility of biopolymer-based films are important quality parameters for many relevant food and pharmaceutical applications [29].

The swelling properties of chitosan films functionalized with TZM nanoparticles are given in Fig. 4. This parameter represents a fundamental criterion of polysaccharide-based materials for biomedical applications, particularly for the development of curative materials [51]. On the first day, significant ($p < 0.05$) differences were detected in the swelling capacity between samples with the nano-TZM (21.09–25.80%) incorporated into the CS-based films (19.79%) in a dose-dependent manner, similar to those obtained with the addition of nano-TiO_2 (22.53–24.77%). Besides, a significant increase ($p < 0.05$) in the swelling index was observed between days 1 and 4 (from 25 to 36%), but the maximum swelling capacity of the films was obtained after 4 days, and no significant differences

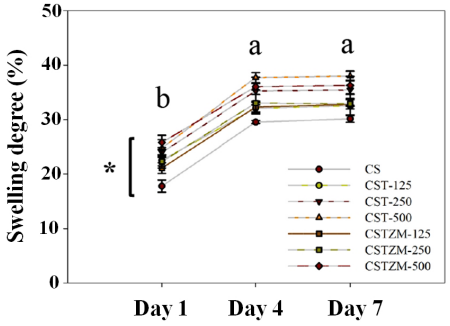

Fig. 4 Swelling degree of chitosan-based films. Different letters indicate significant statistical differences between days ($\alpha = 0.05$), * indicate significant statistical differences between treatments ($\alpha = 0.05$). See also the footnote of Table 1.

($p > 0.05$) were detected on days 4 and 7. Kavitha et al. [27] reported similar trends in a CS-TiO_2 (PBS, pH 7.4 at 25 °C) film after 7 days of evaluation. Likewise, Wiącek et al. [44] reported that CS-TiO_2 films reached a stable equilibrium after 5 days (PBS, pH 5.5 at 25 °C) and that the swelling capacity of the composite is strongly dependent on TiO_2 concentration. Alex et al. [52] informed an increase in the swelling degree of 28% in a TiO_2-Chitosan-chondroitin 4-sulfate composite after 7 days of evaluation (PBS with pH 7.4 at 37 °C). This effect may be related to an increase in the specific surface area of the hybrid composite and an increase in the matrix density by a reinforcement effect of the nano-TZM and its absorptive properties [26, 27]. Materials with a swelling increase between 28 to 40% are suitable for developing curative materials [51, 52].

3.4 Water vapor permeability of chitosan-hybrid films

The water vapor permeability test results of CS-based films with added TZM nanoparticles are given in Fig. 5. A significant ($p < 0.05$) decrease in water vapor permeability (CS = 6.62×10^{-16} g m^{-1} h^{-1} Pa^{-1}) was observed in a dose-dependent manner (from 125 to 500 μg mL^{-1}) when nano-TZM (from 5.28 to 4.33×10^{-16} g m^{-1} h^{-1} Pa^{-1}) and nano-TiO_2 (from 5.56 to 4.89×10^{-16} g m^{-1} h^{-1} Pa^{-1}) were added. A similar trend was reported in CS-based films [38], a mixture of CS-starch [37], a mixture of CS-methyl cellulose [53], a mixture of polysaccharides (*k*-Carrageenan, xanthan gum, and gellan gum) [48], and whey protein isolate [54] films due to the effect of TiO_2 incorporation. Water vapor permeability describes the rate of water molecules passing through the biopolymer film under a given difference in relative humidity [38]. A low water vapor permeability tendency is commonly required for biomedical applications and for the development of food packaging materials [30, 38]. Qu et al. [50] reported that the TiO_2 incorporation in a zein-CS film promotes a decrease in the water vapor permeability (up to 11%) in a dose-dependent response to the addition of TiO_2. The incorporation of inorganic nanoparticles into the polymeric matrix, in particular TiO_2, could improve its water barrier ability [50, 53]. The reduced water vapor permeability values of CS-based films with added mixed oxide-based TiO_2 nanoparticles can be explained as:

1. TZM exhibit lower water solubility in comparison with chitosan,
2. a lower diffusion of the water molecules due to the presence of nanoparticles and an enlarged route through which water molecules had to pass,
3. nano-TZM can interact with functional groups (–OH and –NH) of CS, forming a dense structure that reduces the water sorption of the film, and
4. TZM nanoparticles could also cause changes in the interfacial regions of the resulted film compared to the chitosan film control [37, 38, 40, 49].

Moreover, a significant reduction (35%) in the water vapor permeability rate was obtained using TZM nanoparticles (at 500 μg mL^{-1}) in comparison with nano-TiO_2 (26%) at the same concentration. According to Delgado Alvarado et al. [53], the water vapor permeability rate is influenced by the structural characteristics of the material with which the chitosan films were combined. In this context, nano-TZM could serve as an alternative to enhance the water barrier properties of CS-based films.

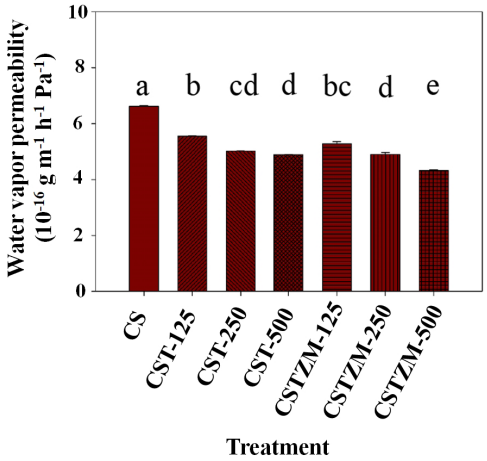

Fig. 5 Water vapor permeability of chitosan-based films. Different letters in each column indicate significant statistical differences between treatments ($\alpha = 0.05$). See also the footnote of Table 1.

3.5 Color attributes and light transmittance of chitosan-TZM hybrid films

As presented in Fig. 1 (b), the CS-based film is transparent and colorless, but in contrast, CSTZM and CST films exhibited reduced visual transparency compared to the control film, followed by a change in color promoted by the addition of inorganic nanoparticles in a dose-dependent response [26]. The visual appearance could be proved by its color values (luminosity, a^*, and b^* coordinates) (Table 2).

A significant decreasing trend ($p < 0.05$) can be observed in luminosity and a^* values for all films with incorporated nano-TZM, followed by a significant increase ($p < 0.05$) in the b^* values compared to the CS and CST films. Similar trends were reported for CS [53], CS-starch [45], and CS-whey protein [55] films with added nano-TiO_2, which

Table 2 Color attributes of chitosan-based films

Film sample	Luminosity	*a**	*b**	Opacity
CS	86.30±0.22^{a}	−0.55±0.07^{a}	4.74±0.55^{f}	0.81
CST-125	78.33±0.61^{b}	−1.80±0.04^{c}	13.93±0.55^{e}	12.19
CST-250	74.33±0.51^{c}	−1.88±0.08^{c}	18.17±0.70^{cd}	15.90
CST-500	71.16±0.57^{d}	−1.43±0.08^{b}	19.74±0.34^{b}	16.43
CSTZM-125	77.35±0.95^{b}	−1.66±0.10^{bc}	17.71±0.21^{d}	15.04
CSTZM-250	77.25±0.38^{b}	−1.72±0.08^{bc}	19.37±0.70^{bc}	16.87
CSTZM-500	71.54±0.63^{d}	−2.20±0.12^{d}	21.22±0.28^{a}	20.46

Values are the average ± standard deviation (n = 3). Different letters in each column indicate significant statistical differences between treatments (α = 0.05). *a**: redness/greenness; *b**: yellowness/blueness. See also the footnote of Table 1.

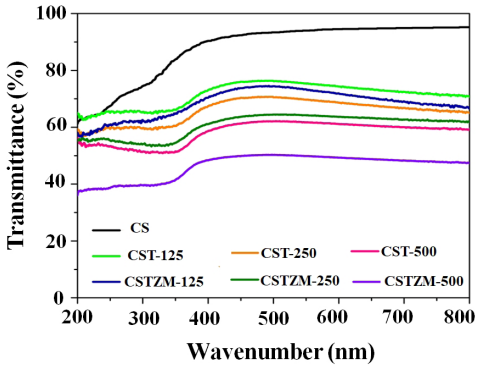

Fig. 6 Transmittance of chitosan-based films

were attributed to the typical characteristics of TiO_2, promoting a decrease in the color values (luminosity, *a**, *b**) [55]. The differences between CSTZM and CST films may be attributable to the presence of Magnesium (MgO color is white to light-yellow) [56]. Additionally, the opacity of the films (CS = 0.81) significantly increased ($p < 0.05$) due to the presence of TZM (14.96–21.42) and TiO_2 (11.17–20.63) nanoparticles in a dose-dependent manner (Table 3), mainly attributed to the scattering of the TiO_2 light capacity [13]. Films with high ultraviolet light-shielding properties are generally required for the preservation of UV-sensitive compounds [26].

In general, the transmittance of CSTZM films (from 63 to 49%) decreased in the ultraviolet-visible region (at 600 nm) as the TZM content increased (from 125 to 500 μg mL^{-1}), and a similar tendency was obtained for CS-based films with added TiO_2 (74 to 68%) compared to CS films, which looks transparent (94.50%) (Fig. 6). The CSTZM-500 film exhibited the highest blocking ability (50.74%) against ultraviolet light radiation compared to CST-500 (38.6%) and CS films (5.5%). This can be attributed to the obstruction of light passage by the TZM nanoparticles, mainly due to the light absorption and scattering ability of the TiO_2 present in the TZM system [26, 48]. Amin and in het Panhius [46] reported a reduction of 30% in the transmittance of chitosan films due to the addition of TiO_2, indicating a good ultraviolet light-barrier property of the hybrid films [29]. The changes in the optical transmittance of biopolymer films have been used to develop packaging materials for diverse industrial applications, particularly because of their ultraviolet light-barrier protection [29, 48].

Table 3 Mechanical properties of chitosan-based films

Treatments	Tensile strength (Pa)	Elongation at break (%)	Elastic modulus (Pa)
CS	4.15±0.25^{cd}	6.96±0.61^{d}	144.24±3.72^{a}
CST-125	3.77±0.31^{de}	47.65±0.20^{c}	6.17±0.35^{c}
CST-250	4.45±0.18^{bc}	46.20±0.68^{c}	11.79±0.60^{b}
CST-500	5.52±0.28^{a}	51.49±0.37^{b}	11.06±0.70^{b}
CSTZM-125	2.05±0.07^{g}	46.55±0.53^{c}	4.11±0.14^{d}
CSTZM-250	3.16±0.28^{f}	52.50±0.36^{b}	5.46±0.33^{c}
CSTZM-500	4.98±0.29^{ab}	56.18±0.54^{a}	6.18±0.29^{c}

Values are the average ± standard deviation. Different letters in each column indicate significant differences between treatments (α = 0.05). See also the footnote of Table 1.

3.6 Thermal behavior of chitosan-TZM hybrid films

The thermal analysis by differential scanning calorimetry of chitosan-based hybrid films with TZM nanoparticles is presented in Fig. 7. The endotherm peaks of CS-based films can be observed in a temperature range of 99.5 to 157.7 °C, which corresponds to the evaporation of water molecules as a nanoparticle concentration function [53].

The endotherm peak of CS-based film occurred at 99.5 °C, which is consistent with previous reports (99.8 °C) [57]. Moreover, the endotherm peak of CSTZM-500 film increased to 157.7 °C, similar to those obtained in CST-500 (152 °C), indicating that high temperature is necessary to cause a free movement of water between the chitosan chains [53, 57]. The thermal properties of biopolymer films reflect their ability to resist decomposition at high temperatures [26]. Grande et al. [57] reported

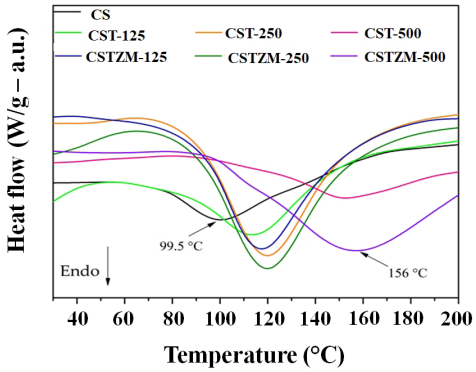

Fig. 7 Thermal behavior of chitosan-based films

a displacement of 14.5 °C in the endotherm peak of chitosan film (99.8 °C) due to the effect of the addition of nano-graphene oxide (CSGO = 114.3 °C), which was attributed to intramolecular interactions between chitosan and graphene oxide. Kochkina and Butikova [58] observed a displacement of 40 °C in the endotherm peak of a corn starch/PVA (190 °C) composite with the addition of nano-TiO_2 at 1% in weight (St/PVA-TiO_2 = 230 °C). Other reports have also confirmed that nano-TiO_2 could efficiently increase the thermal stability of polysaccharide-based films (potato starch, chitosan-potato starch, chitosan-whey protein isolate, and a mixture of *k*-Carrageenan, gellan, and xanthan gums) films [29, 48, 53]. It has been suggested that the thermal stability of biopolymer-based films, particularly of CS-based films, is increased as a result of the incorporation of nano-TiO_2, associated with its ability to form chemical interactions in the amine and hydroxyl groups of the chitosan structure. Consequently, most of the water molecules (water can act as a plasticizer agent in CS-based films) are bonded to –OH groups of chitosan that have a high capacity to form hydrogen bonds, needing greater temperature to remove them [53, 57]. Furthermore, Jbeli et al. [59] reported that the combined addition of TiO_2 and ZnS enhanced the thermal strength of CS-based films compared to the CSTiO_2 films due to the synergistic effect between the two inorganic compounds. Our results suggest that the incorporation of ZnO and MgO into the nano-TZM ternary system and then added to the CS-based films could hold up its degradation rate [21].

3.7 Mechanical properties of hybrid CS-based films

Table 3 shows the effect of adding TZM on the tensile strength, elongation at break, and elastic modulus of the CS-based films. Significant ($p < 0.05$) differences were observed between treatments in elongation at break, tensile strength, and elastic modulus properties in a concentration-dependent manner with better performance at higher concentrations of TZM. Elongation at break and tensile strength of the CS-based films (6.96% and 4.15 kPa, respectively) improved with the incorporation (500 µg mL^{-1}) of TZM (56.18% and 4.98 kPa, respectively), similar to those observed by adding TiO_2 (51.49% and 5.52 kPa, respectively) nanoparticles. These results are in agreement with those of Qu et al. [50], who reported that the incorporation of nano-TiO_2 in the zein/chitosan films resulted in tensile strength reinforcement (from 22 to 28 MPa) and elongation at break increase (40%). The feasibility of film materials and their potential applications are mainly determined by their mechanical properties [26, 60]. Siripatrawan and Kaewklin [38] reported an increase in the tensile strength of CS-based films (from 11 to 16 MPa) due to the effect of the TiO_2 incorporation with a decrease in the elongation at break (less than 10%) compared to the control film. It has been reported that nano-TiO_2 can act as a reinforcement agent in CS-based films, improving their mechanical properties, but these effects depend on the nano-TiO_2 concentration [3, 5]. Additionally, the elastic modulus of chitosan films (144.24 kPa) decreased due to the presence of TZM (6.18 to 4.11 kPa) and TiO_2 (11.06 to 6.17 kPa) nanoparticles in a dose-dependent response. According to Delgado Alvarado et al. [53], the film will be less rigid and more flexible at low elastic modulus values. In this context, the CSTZM-500 film is more flexible than the chitosan and similar to CST-500 films, an appropriate property for polysaccharide-based materials [61]. The reinforcement effect of TiO_2 in the chitosan matrix has been extensively investigated to develop hybrid materials with potential industrial applications [3, 5]. In this context, nano-TZM could be used as a chitosan reinforcement agent to make hybrid composites.

3.8 Structural and morphological studies of hybrid CS-based films

The X-ray diffraction patterns of the CSTZM films are presented in Fig. 8. The characteristic diffraction peak of CS-based film appears at 20.7° (2θ) with a completely amorphous character [62]. The diffractograms of the CS-based films with TZM (CSTZM-125, CSTZM-250, and CSTZM-500) and TiO_2 (CST-125, CST-250, and CST-500) nanoparticles showed diffraction signals at 2θ = 25.3° with a Miller index of (101), associated with the anatase phase of TiO_2 (JCPDS 21–1272). These results are consistent with previous reports on CS-based films incorporated with

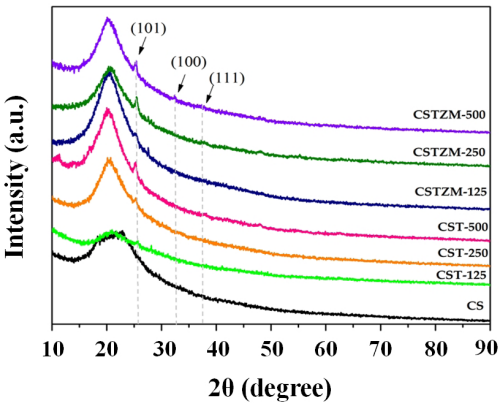

Fig. 8 Effect of TiO_2-ZnO-MgO (TZM) nanoparticles concentration on the X-ray diffraction of chitosan-based films

nano-TiO_2 [13, 27, 61]. In addition, the CSTZM-500 presented a characteristic diffraction peak of ZnO ($2\theta = 31.7°$) and MgO ($2\theta = 37.5°$) structure [21]. It has been reported that the integration of TiO_2 with chitosan occurs in the amorphous region of the biopolymer, promoting changes in the diffraction signal at around 20.7° [13, 27, 38].

The Fourier transform infrared (FTIR) spectra of the CS-based films functionalized with TZM nanoparticles are shown in Fig. 9. The CS-FTIR spectra are consistent with previous reports [38, 63]. Absorption bands from 3500 to 3000 cm^{-1} were observed. It has been reported that the available functional groups ($–NH_2$ and –OH) in the chitosan structure are responsible for the interaction between components through a coordination bond between the nitrogen present in the $–NH_2$ group and TiO_2 (3450 cm^{-1} and 1537 cm^{-1}), which is considered as an active site for the adsorption of inorganic and/or organic compounds [64, 65]. Saravanan et al. [66] mentioned that the stretching bands at 3350 cm^{-1} and 2921 cm^{-1} attributed to the C–O, $–NH_2$, –OH groups interacting with the nano-TiO_2, promoting the formation of hybrid composite (CSTZM) through electrostatic interactions of N–H–O–Ti bonds. Likewise, the absorption bands at 1643 cm^{-1} (C=O stretching), 1537 cm^{-1} (N–H bending), and 1408 cm^{-1} (C–H bending) were attributed to the $–NH_2$ functional group [65, 66], while the absorption band around 1072 cm^{-1} (C–O–C stretching) was ascribed to the acetamide groups of chitosan [38]. The band of about 1029 cm^{-1} (Ti–O–C bond) suggests that the chitosan and nano-TZM have chemically interacted and was not only a physical saturation of nano-TZM into the polymeric matrix [67]. The bands at 620 to 550 cm^{-1} regions are ascribed to the Ti–O, Zn–O, and Mg–O bonds [38]. It has been reported that the functionalization of chitosan with TiO_2:Cu doped did not alter the typical structure of chitosan [20], suggesting that the incorporation of a ternary system (TZM) did not change the typical structure of chitosan.

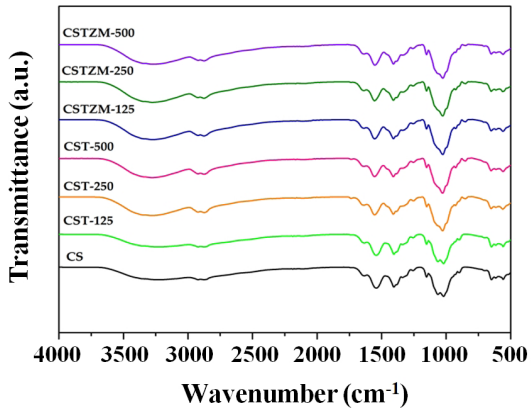

Fig. 9 Effect of TiO_2-ZnO-MgO (TZM) nanoparticles concentration on the FTIR spectra of chitosan-based films

3.9 Principal component analysis and hierarchical cluster analysis

Advanced statistical tools such as principal component analysis and hierarchical cluster analysis are widely used in biopolymer film characterization. These tools include the combined effect of different edible (locust bean gum and *k*-carrageenan) materials on their physicochemical properties [68], as well as to evaluate the effect of starch concentration on the functional properties of films [69]. Principal component analysis was used to estimate the interrelationship among variables and chitosan-based films (Fig. 10). The first two principal components (PC) 1 and 2 explained 92.26% of the total variance (76.03% for PC1 and 16.23% for PC2). The physicochemical, mechanical,

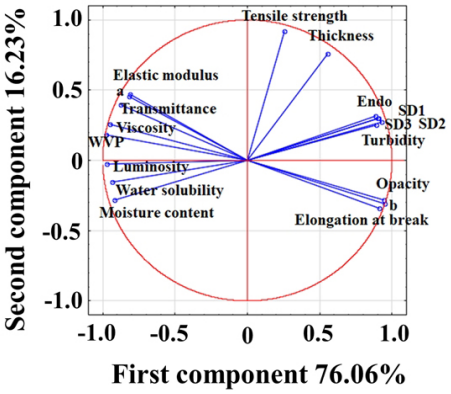

(a)

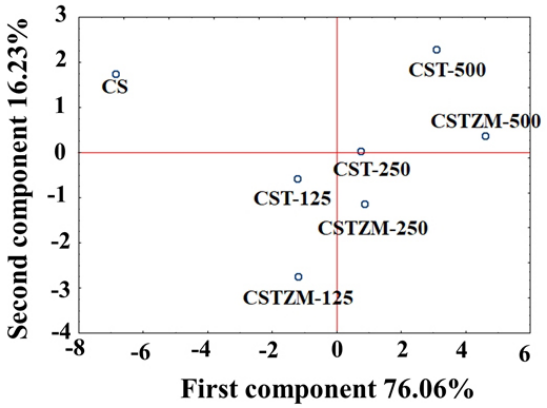

(b)

Fig. 10 Principal component analysis (*PCA*) plots of CS-based films adding TiO_2-ZnO-MgO (TZM) nanoparticles; location of different physicochemical, optical, mechanical, and thermal properties a) and location of different treatments b). *WVP*: water vapor permeability; *SD*: swelling degree

and optical properties of the films are given in Fig. 10 (a), and the graph location of chitosan-based films (CS, CST, and CSTZM) is shown in Fig. 10 (b). The scattergram in Fig. 10 (a) shows the score values (projected in PC1 and PC2 planes and from positive to negative) of all film properties, where opacity (0.948), *b** value (0.943), elongation at break (0.913), thermal stability (endotherm peak) (0.903), swelling degree (*SD*1 = 0.931, *SD*2 = 0.907, *SD*3 = 0.888), and film-forming solution turbidity (0.889) tend to increase, while luminosity (−0.971), water vapor permeability (−0.976), film-forming solution viscosity (−0.949), water solubility (−0.932), moisture content (−0.917), transmittance (−0.877), *a** value (−0.816), and elastic modulus (−0.811) tend to decrease. Furthermore, there exists a differentiation among CS-based films with (TZM and TiO_2) and without nanoparticles added (Fig. 10 (b)). According to the factor coordinates (from negative to positive values of PC1), CS films (−6.862) showed higher differences than the films with added TZM or TiO_2 nanoparticles. CSTZM-125 (−1.21), CST-125 (−1.22), CST-250 (0.743) and CSTZM-250 (0.860) have a closer relationship while the highest score values were obtained from both CST-500 (3.093) and CSTZM-500 (4.605) films. These results demonstrated the relationship between the physicochemical, mechanical, optical, and thermal properties of chitosan-based films functionalized with TZM [70], where the CSTZM-500 films exhibited better properties than the other CS-based films with or without added nanoparticles.

Additionally, hierarchical cluster analysis was carried out and presented as a tree diagram in Fig. 11, where films with similar characteristics are grouped within the same cluster as a contrast; if similarities decreased, other subgroups were formed. CSTZM-500 (first cluster) is different from other CS-based films. A second group consists of CST-500, CSTZM-250, CST-250, CSTZM-125, and CST-125, while a third group includes CS-based films. Thus, the incorporation of TZM (at 500 μg mL^{-1}) nanoparticles improves the technological properties of CS-based films.

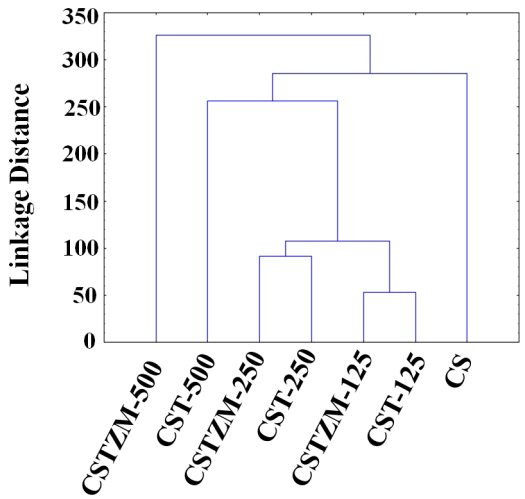

Fig. 11 Hierarchical cluster of CS-based films

3.10 Toxicity assay with *Artemia salina*

The toxicity status of CSTZM-500 hybrid film was investigated using the *Artemia salina* model, a simple, fast, reliable, and low-cost method conducted to evaluate the preliminary toxicity level of any organic and inorganic compound (alone or combined) [36]. The percentage of survival values of *A. salina* in the presence of CSTZM-500 are listed in Table 4. In the in vivo acute toxicity test using *A. salina* larvae, CS-based film did not show toxicity against *A. salina* larvae (100% survival) at the evaluated concentrations (0.5, 1, 2, and 4 mg mL^{-1}). These findings agree with those of Parvez et al. [33], who reported that chitosan films were not acutely toxic to *A. salina* at concentrations of 4 mg mL^{-1} or lower. The CSTZM-500 hybrid film exhibited percentages of survival > 93% at concentrations of 4 mg mL^{-1}, and no mortality was observed at concentrations < 4 mg mL^{-1} (100% survival), which were similar to those observed in the CST hybrid films. Gonçalves et al. [69] reported that chitosan combined with $ZnSO_4$ did not show toxic effects on *A. salina*, while a low sign of toxicity using chitosan-$AgNO_3$ and chitosan-Cu composites were reported. It has been reported that chitosan and its derivates incorporated with ceftazidime drug did not show significant toxicological effects

Table 4 Effect of chitosan-based films on *Artemia salina* larvae

Treatments (code)	Film concentration (mg mL^{-1})	Larvae survival (%)
Saline solution (C-)		100
DMSO (mL mL^{-1})	0.5	0
CS	0.5	100
	1	100
	2	100
	4	100
CST-500	0.5	100
	1	100
	2	100
	4	93.33
CSTZM-500	0.5	100
	1	100
	2	100
	4	93.33

(17 to 20% of dead nauplii) in *A. salina* at 10 mg mL^{-1} [35]. Furthermore, Chitosan-TiO_2 did not exhibit toxicological or adverse effects on osteoblast-like cells, fibroblast cells, and human mesenchymal stem cells [51, 71]. These results indicated that CSTZM-500 was non-toxic to the crustacean model and could be potentially used in the development of materials for diverse industrial applications.

4 Conclusions

The addition of TiO_2-ZnO-MgO (TZM) mixed oxide nanoparticles to chitosan films improved water vapor permeability, water-solubility, swelling degree, elastic modulus, elongation at break, tensile strength, and thermal properties but decreased the optical transmittance in a dose-dependent response. X-ray diffraction and Fourier transform infrared studies confirmed the interactions between chitosan and TZM nanoparticles, which were responsible for the improved properties of the chitosan films. Principal component and hierarchical cluster analysis demonstrated the relationship between all studied properties in hybrid CS-based films with added mixed oxide nanoparticles, where the CSTZM-500 film exhibited better properties compared to those obtained with chitosan films with added pure nano-TiO_2 or the chitosan alone. CSTZM-500 film has the potential to be used as a functional material for diverse industrial applications, according to all the physicochemical, optical, mechanical, and structural properties, with no toxic effects on *A. salina*. However, further studies are still needed to evaluate the safe use and implementation of this kind of material.

Acknowledgments

The authors gratefully acknowledge the funding obtained from National Technologic of Mexico (Grant No. 10474.21-P), the financial support received as a scholarship (702634) from CONACYT-Mexico, and technical support from Mr. Sergio Oliva and Dr. Martín Flores for the use of the XRD equipment at the University Center for Exact Sciences and Engineering of the University of Guadalajara.

References

[1] Amri, N., Ghemati, D., Bouguettaya, N., Aliouche, D. "Swelling Kinetics and Rheological Behavior of Chitosan-PVA/Montmorillonite Hybrid Polymers", Periodica Polytechnica Chemical Engineering, 63(1), pp. 179–189, 2019. https://doi.org/10.3311/PPch.12227

[2] Kulyk, K., Ishchenko, V., Palyanytsya, B., Khylya, V., Borysenko, M., Kulyk, T. "A TPD-MS study of the interaction of coumarins and their heterocyclic derivatives with a surface of fumed silica and nanosized oxides CeO_2/SiO_2, TiO_2/SiO_2, Al_2O_3/SiO_2", Journal of Mass Spectrometry, 45(7), pp. 750–761, 2010. https://doi.org/10.1002/jms.1765

[3] Anaya-Esparza, L. M., Villagrán-de la Mora, Z., Ruvalcaba-Gómez, J. M., Romero-Toledo, R., Sandoval-Contreras, T., Aguilera-Aguirre, S., Montalvo-González, E., Pérez-Larios, A. "Use of Titanium Dioxide (TiO_2) Nanoparticles as Reinforcement Agent of Polysaccharide-Based Materials", Processes, 8(11), Article No.: 1395, 2020. https://doi.org/10.3390/pr8111395

[4] Ikhaddalene, S., Zibouche, F., Ponton, A., Irekti, A., Carn, F. "Synthesis and Rheological Properties of Magnetic Chitosan Hydrogel", Periodica Polytechnica Chemical Engineering, 65(3), pp. 378–388, 2021. https://doi.org/10.3311/PPch.17148

[5] Anaya-Esparza, L. M., Ruvalcaba-Gómez, J. M., Maytorena-Verdugo, C. I., González-Silva, N., Romero-Toledo, R., Aguilera-Aguirre, S., Pérez-Larios, A., Montalvo-González, E. "Chitosan-TiO_2: A Versatile Hybrid Composite", Materials, 13(4), Article No.: 811, 2020. https://doi.org/10.3390/ma13040811

[6] Rokhati, N., Susanto, H., Haryani, K., Pramudono, B. "Enhanced Enzymatic Hydrolysis of Chitosan by Surfactant Addition", Periodica Polytechnica Chemical Engineering, 62(3), pp. 286–291, 2018. https://doi.org/10.3311/PPch.11142

[7] Nagarajan, V., Ganesan, R., Govindan, S., Govindaraj, P. "Adsorptive Removal of As(V) from Aqueous Solution onto Steel Slag Recovered Iron – Chitosan Composite: Response Surface Modeling and Kinetics", Periodica Polytechnica Chemical Engineering, 65(2), pp. 270–280, 2021. https://doi.org/10.3311/PPch.17208

[8] Phattepur, H., Bychapur Siddaiah, G., Ganganagappa, N. "Synthesis and Characterisation of Mesoporous TiO_2 Nanoparticles by Novel Surfactant Assisted Sol-gel Method for the Degradation of Organic Compounds", Periodica Polytechnica Chemical Engineering, 63(1), pp. 85–95, 2019. https://doi.org/10.3311/PPch.11789

[9] U.S. Food and Drug Administration "Part 73 – Listing of Color Additives Exempt from Certification", In: Code of Federal Regulations – Title 21 – Food and Drugs, Vol. 1, Department of Health and Human Services, U.S. Food and Drug Administration, New Hampshire, MD, USA, Paper No.: 21CFR73.575. [online] Available at: https://www.accessdata.fda.gov/scripts/cdrh/cfdocs/cfcfr/cfrsearch.cfm?fr=73.575 [Accessed: 22 November 2021]

[10] EFSA Panel on Food Additives and Flavourings (FAF), Younes, M., Aquilina, G., Castle, L., Engel, K.-H., Fowler, P., Frutos Fernandez, M. J., Fürst, P., Gundert-Remy, U., Gürtler, R., Husøy, T., …, Wright, M. "Safety assessment of titanium dioxide (E171) as a food additive", EFSA Journal, 19(5), Article No.: 6585, 2021. https://doi.org/10.2903/j.efsa.2021.6585

[11] U.S. Food and Drug Administration "Part 175 - Indirect Food Additives: Adhesives and Components of Coatings", In: Code of Federal Regulations – Title 21 – Food and Drugs, Vol. 3, Department of Health and Human Services, U.S. Food and Drug Administration, New Hampshire, MD, USA, Paper No.: 21CFR175.300. [online] Available at: https://www.accessdata.fda.gov/scripts/cdrh/cfdocs/cfcfr/cfrsearch.cfm?fr=175.300 [Accessed: 22 November 2021]

[12] Díaz-Visurraga, J., Meléndez, M. F., García, A., Paulraj, M., Cárdenas, G. "Semitransparent chitosan-TiO_2 nanotubes composite film for food package applications", Journal of Applied Polymer Science, 116, pp. 3503–3515, 2010. https://doi.org/10.1002/app.31881

[13] Zhang, X., Xiao, G., Wang, Y., Zhao, Y., Su, H., Tan, T. "Preparation of chitosan-TiO_2 composite film with efficient antimicrobial activities under visible light for food packaging applications", Carbohydrate Polymers, 169, pp. 101–107, 2017. https://doi.org/10.1016/j.carbpol.2017.03.073

[14] Razzaz, A., Ghorban, S., Hosayni, L., Irani, M., Aliabadi, M. "Chitosan nanofibers functionalized by TiO_2 nanoparticles for the removal of heavy metal ions", Journal of the Taiwan Institute of Chemical Engineers, 58, pp. 333–343, 2016. https://doi.org/10.1016/j.jtice.2015.06.003

[15] Safari, M., Ghiaci, M., Jafari-Asl, M., Ensafi, A. A. "Nanohybrid organic-inorganic chitosan/dopamine/TiO_2 composites with controlled drug-delivery properties", Applied Surface Science, 342, pp. 26–33, 2015. https://doi.org/10.1016/j.apsusc.2015.03.028

[16] Kaewklin, P., Siripatrawan, U., Suwanagul, A., Lee, Y. S. "Active packaging from chitosan-titanium dioxide nanocomposite film for prolonging storage life of tomato fruit", International Journal of Biological Macromolecules, 112, pp. 523–529, 2018. https://doi.org/10.1016/j.ijbiomac.2018.01.124

[17] Pincus, L. N., Melnikov, F., Yamani, J. S., Zimmerman, J. B. "Multifunctional photoactive and selective adsorbent for arsenite and arsenate: Evaluation of nano titanium dioxide-enabled chitosan cross-linked with copper", Journal of Hazardous Materials, 358, pp. 145–154, 2018. https://doi.org/10.1016/j.jhazmat.2018.06.033

[18] Xiao, G., Zhao, Y., Li, L., Pratt, J. O., Su, H., Tan, T. "Facile synthesis of dispersed Ag nanoparticles on chitosan-TiO_2 composites as recyclable nanocatalysts for 4-nitrophenol reduction", Nanotechnology, 29(15), Article No.: 155601, 2018. https://doi.org/10.1088/1361-6528/aaac74

[19] Xiao, G., Zhang, X., Zhang, W., Zhang, S., Su, H., Tan, T. "Visible-light-mediated synergistic photocatalytic antimicrobial effects and mechanism of Ag-nanoparticles@chitosan–TiO_2 organic–inorganic composites for water disinfection", Applied Catalysis B: Environmental, 170–171, pp. 255–262, 2015. https://doi.org/10.1016/j.apcatb.2015.01.042

[20] Raut, A. V., Yadav, H. M., Gnanamani, A., Pushpavanam, S., Pawar, S. H. "Synthesis and characterization of chitosan-TiO_2:Cu nanocomposite and their enhanced antimicrobial activity with visible light", Colloids and Surfaces B: Biointerfaces, 148, pp. 566–575, 2016. https://doi.org/10.1016/j.colsurfb.2016.09.028

[21] Anaya-Esparza, L. M., Montalvo-González, E., González-Silva, N., Méndez-Robles, M. D., Romero-Toledo, R., Yahia, E. M., Pérez-Larios, A. "Synthesis and Characterization of TiO_2-ZnO-MgO Mixed Oxide and Their Antibacterial Activity", Materials, 12(5), Article No.: 698, 2019. https://doi.org/10.3390/ma12050698

[22] Anaya-Esparza, L. M., González-Silva, N., Yahia, E. M., González-Vargas, O. A., Montalvo-González, E., Pérez-Larios, A. "Effect of TiO_2-ZnO-MgO Mixed Oxide on Microbial Growth and Toxicity against *Artemia salina*", Nanomaterials, 9(7), Article No.: 992, 2019. https://doi.org/10.3390/nano9070992

[23] Yong, H., Wang, X., Bai, R., Miao, Z., Zhang, X., Liu, J. "Development of antioxidant and intelligent pH-sensing packaging films by incorporating purple-fleshed sweet potato extract into chitosan matrix", Food Hydrocolloids, 90, pp. 216–224, 2019. https://doi.org/10.1016/j.foodhyd.2018.12.015

[24] Tang, Y., Hu, X., Zhang, X., Guo, D., Zhang, J., Kong, F. "Chitosan/titanium dioxide nanocomposite coatings: Rheological behavior and surface application to cellulosic paper", Carbohydrate Polymers, 151, pp. 752–759, 2016. https://doi.org/10.1016/j.carbpol.2016.06.023

[25] Chen, Y.-C., Wang, C.-H., Lai, L.-S., Lin, K.-W. "Rheological Properties of Chitosan and its Interaction with Porcine Myofibrillar Proteins as Influenced by Chitosan's Degree of Deacetylation and Concentration", Journal of Food Science, 68(3), pp. 826–831, 2003. https://doi.org/10.1111/j.1365-2621.2003.tb08250.x

[26] Zhang, X., Liu, Y., Yong, H., Qin, Y., Liu, J., Liu, J. "Development of multifunctional food packaging films based on chitosan, TiO_2 nanoparticles and anthocyanin-rich black plum peel extract", Food Hydrocolloids, 94, pp. 80–92, 2019. https://doi.org/10.1016/j.foodhyd.2019.03.009

[27] Kavitha, K., Sutha, S., Prabhu, M., Rajendran, V., Jayakumar, T. "*In situ* synthesized novel biocompatible titania–chitosan nanocomposites with high surface area and antibacterial activity", Carbohydrate Polymers, 93(2), pp. 731–739, 2013. https://doi.org/10.1016/j.carbpol.2012.12.031

[28] ASTM "ASTM E96-95 Standard Test Method for Water Vapor Transmission of Materials", ASTM International, West Conshohocken, PA, USA, 1995.

[29] Oleyaei, S. A., Zahedi, Y., Ghanbarzadeh, B., Moayedi, A. A. "Modification of physicochemical and thermal properties of starch films by incorporation of TiO_2 nanoparticles", International Journal of Biological Macromolecules, 89, pp. 256–264, 2016. https://doi.org/10.1016/j.ijbiomac.2016.04.078

[30] Nouri, L., Mohammadi Nafchi, A. "Antibacterial, mechanical, and barrier properties of sago starch film incorporated with betel leaves extract", International Journal of Biological Macromolecules, 66, pp. 254–259, 2014. https://doi.org/10.1016/j.ijbiomac.2014.02.044

[31] ASTM "ASTM D882-95a Standard Test Method for Tensile Properties of Thin Plastic Sheeting", ASTM International, West Conshohocken, PA, USA, 1995.

[32] Contreras-Cortés, A. G., Almendariz-Tapia, F. J., Gómez-Álvarez, A., Burgos-Hernández, A., Luque-Alcaraz, A. G., Rodríguez-Félix, F., Quevedo-López, M. A., Plascencia-Jatomea, M. "Toxicological Assessment of Cross-Linked Beads of Chitosan-Alginate and *Aspergillus australensis* Biomass, with Efficiency as Biosorbent for Copper Removal", Polymers, 11(2), Article No.: 222, 2019. https://doi.org/10.3390/polym11020222

[33] Parvez, S., Rahman, M. M., Khan, M. A., Khan, M. A. H., Islam, J. M. M., Ahmed, M., Rahman, M. F., Ahmed, B. "Preparation and characterization of artificial skin using chitosan and gelatin composites for potential biomedical application", Polymer Bulletin, 69(6), pp. 715–731, 2012. https://doi.org/10.1007/s00289-012-0761-7

[34] Freire, P. L. L., Albuquerque, A. J. R., Farias, I. A. P., da Silva, T. G., Aguiar, J. S., Galembeck, A., Flores, M. A. P., Sampaio, F. C., Stamford, T. C. M., Rosenblatt, A. "Antimicrobial and cytotoxicity evaluation of colloidal chitosan – silver nanoparticles – fluoride nanocomposites", International Journal of Biological Macromolecules, 93(Part A), pp. 896–903, 2016. https://doi.org/10.1016/j.ijbiomac.2016.09.052

[35] Pereira, L. A., da Silva Reis, L., Batista, F. A., Mendes, A. N., Osajima, J. A., Silva-Filho, E. C. "Biological properties of chitosan derivatives associated with the ceftazidime drug", Carbohydrate Polymers, 222, Article No.: 115002, 2019. https://doi.org/10.1016/j.carbpol.2019.115002

[36] Kurniasih, M., Purwati, Dewi, R. S. "Toxicity tests, antioxidant activity, and antimicrobial activity of chitosan", IOP Conference Series: Materials Science Engineering, 349, Article No.: 012037, 2018. https://doi.org/10.1088/1757-899X/349/1/012037

[37] Li, W., Zheng, K., Chen, H., Feng, S., Wang, W., Qin, C. "Influence of Nano Titanium Dioxide and Clove Oil on Chitosan–Starch Film Characteristics", Polymers, 11(9), Article No.: 1418, 2019. https://doi.org/10.3390/polym11091418

[38] Siripatrawan, U., Kaewklin, P. "Fabrication and characterization of chitosan-titanium dioxide nanocomposite film as ethylene scavenging and antimicrobial active food packaging", Food Hydrocolloids, 84, pp. 125–134, 2018. https://doi.org/10.1016/j.foodhyd.2018.04.049

[39] Wu, C., Tian, J., Li, S., Wu, T., Hu, Y., Chen, S., Sugawara, T., Ye, X. "Structural properties of films and rheology of film-forming solutions of chitosan gallate for food packaging", Carbohydrate Polymers, 146, pp. 10–19, 2016. https://doi.org/10.1016/j.carbpol.2016.03.027

[40] Li, Y., Yokoyama, W., Wu, J., Ma, J., Zhong, F. "Properties of edible films based on pullulan-chitosan blended film-forming solutions at different pH", RSC Advances, 5(128), pp. 105844–105850, 2015. https://doi.org/10.1039/C5RA21876D

[41] Al-Sagheer, F. A., Merchant, S. "Visco-elastic properties of chitosan-titania nano-composites", Carbohydrate Polymers, 85(2), pp. 356–362, 2011. https://doi.org/10.1016/j.carbpol.2011.02.032

[42] Li, Q., Su, H., Tan, T. "Synthesis of ion-imprinted chitosan-TiO_2 adsorbent and its multi-functional performances", Biochemical Engineering Journal, 38(2), pp. 212–218, 2008. https://doi.org/10.1016/j.bej.2007.07.007

[43] Abugoch, L. E., Tapia, C., Villamán, M. C., Yazdani-Pedram, M., Díaz-Dosque, M. "Characterization of quinoa protein-chitosan blend edible films", Food Hydrocolloids, 25(5), pp. 879–886, 2011. https://doi.org/10.1016/j.foodhyd.2010.08.008

[44] Wiącek, A. E., Gozdecka, A., Jurak, M. "Physicochemical Characteristics of Chitosan–TiO_2 Biomaterial. 1. Stability and Swelling Properties", Industrial & Engineering Chemistry Research, 57(6), pp. 1859–1870, 2018. https://doi.org/10.1021/acs.iecr.7b04257

[45] González-Calderon, J. A., Vallejo-Montesinos, J., Martínez-Martínez, H. N., Cerecero-Enríquez, R., López-Zamora, L. "Effect of Chemical Modification of Titanium Dioxide Particles via Silanization under Properties of Chitosan/Potato-starch Films", Revista Mexicana de Ingeniería Química, 18(3), pp. 913–927, 2019. https://doi.org/10.24275/uam/izt/dcbi/revmexingquim/2019v18n3/GonzalezC

[46] Amin, K. A. M., in het Panhius, M. "Reinforced Materials Based on Chitosan, TiO_2 and Ag Composites", Polymers, 4(1), pp. 590–599, 2012. https://doi.org/10.3390/polym4010590

[47] Lian, Z., Zhang, Y., Zhao, Y. "Nano-TiO_2 particles and high hydrostatic pressure treatment for improving functionality of polyvinyl alcohol and chitosan composite films and nano-TiO_2 migration from film matrix in food simulants", Innovative Food Science & Emerging Technologies, 33, pp. 145–153, 2016. https://doi.org/10.1016/j.ifset.2015.10.008

[48] Balasubramanian, R., Kim, S. S., Lee, J., Lee, J. "Effect of TiO_2 on highly elastic, stretchable UV protective nanocomposite films formed by using a combination of *k*-Carrageenan, xanthan gum and gellan gum", International Journal of Biological Macromolecules, 123, pp. 1020–1027, 2019. https://doi.org/10.1016/j.ijbiomac.2018.11.151

[49] Vallejo-Montesinos, J., Gámez-Cordero, J., Zarraga, R., Pérez Pérez, M. C., Gonzalez-Calderon, J. A. "Influence of the surface modification of titanium dioxide nanoparticles TiO_2 under efficiency of silver nanodots deposition and its effect under the properties of starch-chitosan (SC) films", Polymer Bulletin, 77(1), pp. 107–133, 2020. https://doi.org/10.1007/s00289-019-02740-z

[50] Qu, L., Chen, G., Dong, S., Huo, Y., Yin, Z., Li, S., Chen, Y. "Improved mechanical and antimicrobial properties of zein/chitosan films by adding highly dispersed nano-TiO_2", Industrial Crops and Products, 130, pp. 450–458, 2019. https://doi.org/10.1016/j.indcrop.2018.12.093

[51] Jayakumar, R., Ramachandran, R., Divyarani, V. V., Chennazhi, K. P., Tamura, H., Nair, S. V. "Fabrication of chitin–chitosan/nano TiO_2-composite scaffolds for tissue engineering applications", International Journal of Biological Macromolecules, 48(2), pp. 336–344, 2011. https://doi.org/10.1016/j.ijbiomac.2010.12.010

[52] Alex, M. J., Periasamy, P., Mohan, K., Sekar, S., Prabha, K. K. S., Venkatachalam, R. "*In situ* synthesised TiO_2-chitosan-chondroitin 4–sulphate nanocomposites for bone implant applications", IET Nanobiotechnology, 10(3), pp. 107–113, 2016. https://doi.org/10.1049/iet-nbt.2015.0023

[53] Delgado Alvarado, E., Peña Juárez, M. G., Pérez Pérez, C., Pérez, E., González Calderón, J. A. "Improvement in the dispersion of TiO_2 particles inside Chitosan-Methyl cellulose films by the use of silane coupling agent", Journal of the Mexican Chemical Society, 63(2), pp. 164–168, 2019. https://doi.org/10.29356/jmcs.v63i2.741

[54] Li, Y., Jiang, Y., Liu, F., Ren, F., Zhao, G., Leng, X. "Fabrication and characterization of TiO_2/whey protein isolate nanocomposite film", Food Hydrocolloids, 25(5), pp. 1098–1104, 2011. https://doi.org/10.1016/j.foodhyd.2010.10.006

[55] Zhang, Y., Chen, L., Liu, C., Feng, X., Wei, L., Shao, L. "Self-assembly chitosan/gelatin composite coating on icariin-modified TiO_2 nanotubes for the regulation of osteoblast bioactivity", Materials & Design, 92, pp. 471–479, 2016. https://doi.org/10.1016/j.matdes.2015.12.023

[56] Maurya, A., Bhatia, N. "Microwave Assisted Sol Gel Synthesis of Magnesium Oxide (Mgo)", International Journal of Engineering Research and Development, 13(8), pp. 1–6, 2017. [online] Available at: http://www.ijerd.com/v13i8.html [Accessed: 16 June 2021]

[57] Grande, C. D., Mangadlao, J., Fan, J., Leon, A., Delgado-Ospina, J., Rojas, J. G., Rodrigues, D. F., Advincula, R. "Chitosan Cross-Linked Graphene Oxide Nanocomposite Films with Antimicrobial Activity for Application in Food Industry", Macromolecular Symposia, 374(1), Article No.: 1600114, 2017. https://doi.org/10.1002/masy.201600114

[58] Kochkina, N. E., Butikova, O. A. "Effect of fibrous TiO_2 filler on the structural, mechanical, barrier and optical characteristics of biodegradable maize starch/PVA composite films", International Journal of Biological Macromolecules, 139, pp. 431–439, 2019. https://doi.org/10.1016/j.ijbiomac.2019.07.213

[59] Jbeli, A., Ferraria, A. M., Botelho do Rego, A. M., Boufi, S., Bouattour, S. "Hybrid chitosan-TiO_2/ZnS prepared under mild conditions with visible-light driven photocatalytic activity", International Journal of Biological Macromolecules, 116, pp. 1098–1104, 2018. https://doi.org/10.1016/j.ijbiomac.2018.05.141

[60] Pereira dos Santos, E., Nicácio, P. H. M., Coêlho Barbosa, F., Nunes da Silva, H., Andrade, A. L. S., Lia Fook, M. V., de Lima Silva, S. M., Farias Leite, I. "Chitosan/Essential Oils Formulations for Potential Use as Wound Dressing: Physical and Antimicrobial Properties", Materials, 12(14), Article No.: 2223, 2019. https://doi.org/10.3390/ma12142223

[61] Kamal, T., Anwar, Y., Khan, S. B., Chani, M. T. S., Asiri, A. M. "Dye adsorption and bactericidal properties of TiO_2/chitosan coating layer", Carbohydrate Polymers, 148, pp. 153–160, 2016. https://doi.org/10.1016/j.carbpol.2016.04.042

[62] Kosowska, K., Domalik-Pyzik, P., Krok-Borkowicz, M., Chłopek, J. "Synthesis and Characterization of Chitosan/Reduced Graphene Oxide Hybrid Composites", Materials, 12(13), Article No.: 2077, 2019. https://doi.org/10.3390/ma12132077

[63] Habiba, U., Joo, T. C., Siddique, T. A., Salleh, A., Ang, B. C., Afifi, A. M. "Effect of degree of deacetylation of chitosan on adsorption capacity and reusability of chitosan/polyvinyl alcohol/TiO_2 nano composite", International Journal of Biological Macromolecules, 104(Part A), pp. 1133–1142, 2017. https://doi.org/10.1016/j.ijbiomac.2017.07.007

[64] Mohandas, A., Deepthi, S., Biswas, R., Jayakumar, R. "Chitosan based metallic nanocomposite scaffolds as antimicrobial wound dressings", Bioactive Materials, 3(3), pp. 267–277, 2018. https://doi.org/10.1016/j.bioactmat.2017.11.003

[65] Zainal, Z., Hui, L. K., Hussein, M. Z., Abdullah, A. H., Hamadneh, I. R. "Characterization of TiO_2–Chitosan/Glass photocatalyst for the removal of a monoazo dye via photodegradation–adsorption process", Journal of Hazardous Materials, 164(1), pp. 138–145, 2009. https://doi.org/10.1016/j.jhazmat.2008.07.154

[66] Saravanan, R., Aviles, J., Gracia, F., Mosquera, E., Gupta, V. K. "Crystallinity and lowering band gap induced visible light photocatalytic activity of TiO_2/CS (Chitosan) nanocomposites", International Journal of Biological Macromolecules, 109, pp. 1239–1245, 2018. https://doi.org/10.1016/j.ijbiomac.2017.11.125

[67] Farzana, M. H., Meenakshi, S. "Synergistic Effect of Chitosan and Titanium Dioxide on the Removal of Toxic Dyes by the Photodegradation Technique", Industrial & Engineering Chemistry Research, 53(1), pp. 55–63, 2014. https://doi.org/10.1021/ie402347g

[68] Martins, J. T., Cerqueira, M. A., Bourbon, A. I., Pinheiro, A. C., Souza, B. W. S., Vicente, A. A. "Synergistic effects between κ-carrageenan and locust bean gum on physicochemical properties of edible films made thereof", Food Hydrocolloids, 29(2), pp. 280–289, 2012. https://doi.org/10.1016/j.foodhyd.2012.03.004

[69] Gonçalves, R. C., da Silva, D. P., Signini, R., Naves, P. L. F. "Inhibition of bacterial biofilms by carboxymethyl chitosan combined with silver, zinc and copper salts", International Journal of Biological Macromolecules, 105(1), pp. 385–392, 2017. https://doi.org/10.1016/j.ijbiomac.2017.07.048

[70] Vicentini, N. M., Dupuy, N., Leitzelman, M., Cereda, M. P., Sobral, P. J. A. "Prediction of Cassava Starch Edible Film Properties by Chemometric Analysis of Infrared Spectra", Spectroscopy Letters, 38(6), pp. 749–767, 2005. https://doi.org/10.1080/00387010500316080

[71] Peng, C.-C., Yang, M.-H., Chiu, W.-T., Chiu, C.-H., Yang, C.-S., Chen, Y.-W., Chen, K.-C., Peng, R. Y. "Composite Nano-Titanium Oxide–chitosan Artificial Skin Exhibits Strong Wound-Healing Effect – An Approach with Anti-Inflammatory and Bactericidal Kinetics", Macromolecular Bioscience, 8(4), pp. 316–327, 2008. https://doi.org/10.1002/mabi.200700188